MAGNETIC CHARACTERISTICS AND MEASUREMENTS OF FILAMENTARY Nb-Ti WIRE FOR THE SUPERCONDUCTING SUPER COLLIDER

R. B. Goldfarb and R. L. Spomer

Electromagnetic Technology Division
National Institute of Standards and Technology
Boulder, Colorado 80303

ABSTRACT

In synchrotron accelerator applications, such as the Superconducting Super Collider (SSC), superconducting magnets are cycled in magnetic field. Desirable properties of the magnets include field uniformity, field stability with time, small residual field, and fairly small energy losses upon cycling. This paper discusses potential sources of problems in achieving these goals, describes important magnetic characteristics to be considered, and reviews measurement techniques for magnetic evaluation of candidate SSC wires. Instrumentation that might be practical for use in a wire-fabrication environment is described. We report on magnetic measurements of prototype SSC wires and cables and speculate on causes for instability in multipole fields of dipole magnets constructed with such cables.

INTRODUCTION

A typical field cycle for the proposed Superconducting Super Collider (SSC) consists of an initial charge to a full field of 6.6 T, reduction of field to 50 mT, increase to 0.33 T for proton injection, and a slow increase of field to 6.6 T as the proton beam is accelerated.[1] The multifilamentary Nb-Ti cables used in the construction of the superconducting dipole magnets are themselves exposed to the field of adjacent windings, usually approximated as a transverse field. Electromagnetic characteristics of the wires and cables are potential sources of difficulty in meeting magnet specifications. Thus, requirements for the magnet imply design and performance specifications for the wires and cables. In this paper we discuss magnetic parameters useful for evaluating multifilar Nb-Ti superconductor wire and cable for the SSC.

MAGNETIC CHARACTERISTICS

Superconductors under steady-state conditions are lossless except for losses associated with thermally activated flux creep. With transient or ac currents and fields, there are several sources of energy dissipation. These ac losses may be classified according to their mechanism and localization within a wire composed of fine superconducting filaments in a normal-metal matrix.

Advances in Cryogenic Engineering (Materials), Vol. 36
Edited by R. P. Reed and F. R. Fickett
Plenum Press, New York, 1990

In this section we describe ac loss effects that may be detected with magnetic instrumentation. We discuss both time-independent and time-dependent phenomena for the wire and cable, not the dipole magnets made with these elements. Ideally, all of these ac losses should be minimized, subject to the often conflicting requirements of high critical current and stability against propagation of a normal zone (quench).

Time-Independent Effects

Hysteresis. Magnetic hysteresis upon field cycling is a major loss mechanism. Hysteresis loss per field cycle is frequency independent. It arises in type-II superconductors from irreversibility of the penetration of flux vortices and shielding currents resulting from flux pinning in the filament volume and at the filament surface. The energy dissipation *per se* might be viewed as a trivial problem in applications where field is only occasionally cycled. However, large hysteresis leads to large remanent magnetization from trapped flux in the filaments as the applied field is reduced to zero. This remanent magnetization is the source of residual field in a superconducting magnet. Even at low fields, such as the 0.33-T SSC injection field, trapped flux acts as an offset to the field expected from the magnet current. When it is predictable, the residual field may be compensated. Field uniformity is usually achieved by strategic magnet design. However, remanent magnetization due to trapped flux in the superconductor wires makes it difficult to obtain uniform fields at low currents.

Because the ability of a superconductor to pin flux is an essential requirement for high critical current, both small remanent magnetization and small hysteresis may be achieved, not by reducing flux pinning, but by reducing filament diameter, as predicted by the critical state model.[2] Hysteresis loss is generally higher for wire carrying transport current than for an open-circuited sample, with the extra energy provided by the current source, not the field.[3] Hysteresis loss is determined as the enclosed area in a plot of magnetization vs. field. Measurements often are made with field cycled from positive to negative values. The SSC cycle is such that fields are always positive. In typical multifilamentary wires measured in transverse field, positive-field hysteresis loops, with maximum applied fields of 1 T, have about 45% of the loss associated with complete hysteresis loops.

Self-field of transport current. When transport current changes, moving self-field lines dissipate energy.[4] The use of small-diameter wires reduces these virtually hysteretic losses. In fine-filament wires, the self-field loss may be greater than the magnetic hysteresis loss. In accelerator applications, cabling with fully transposed strands reduces self-field loss; simple twisted strands would still have a large self-field. Three methods of transposition are twisted rope, woven braid, and flattened twisted cable. The last is planned for the SSC, but it results in mechanical damage to the cable corners with a local reduction in critical current.[5]

Coupling between filaments. There are two time-independent sources of filament coupling. One is simply interfilament contact arising from metallurgical problems in processing. Coupled filaments act as a single filament of large diameter, with its associated problems. The second is interfilamentary coupling by the proximity effect when filament spacing is on the order of the coherence length. This type of coupling is important for wires with closely spaced fine filaments. The addition of impurities, such as Ni or Mn, to the matrix material is often effective in reducing the coupling.[6] In any event, proximity-effect coupling is disrupted when magnetic fields approach the effective critical field of the coupling medium. The losses associated with time-independent filament coupling are hysteretic.

Time-Dependent Effects

Coupling between filaments. An important coupling arises from eddy currents driven by voltages induced by a changing applied field. Coupling loss is caused by the transfer of current between filaments and dissipation within the matrix. This relaxation phenomenon leads to time-varying magnetization and field instability of the magnet. It may be reduced by transposing the filaments, approximated by twisting the wire, during manufacture.[7] This decreases the longitudinal distance over which the transverse coupling currents can flow. Other ways to reduce coupling are by increasing the resistivity of the Cu matrix and by increasing the distance between filaments. The former strategy is consistent with other wire requirements provided the stability of the conductor is not impaired.

Flux creep. Flux creep consists of thermally activated jumps of bundles of flux vortices between pinning sites at constant field. Flux creep causes slow changes in magnetization and, in a superconducting magnet, changes in magnet field. Flux creep is often ignored in strong-pinning superconducting materials. In particular, the critical state model assumes that there is no flux creep.[2] However, flux creep has been found to be a problem in accelerator dipole magnets.[8-10] The activation energy for flux creep is reduced by the Lorentz force of the applied field on vortex currents.[11] Flux flow results as a limiting case when flux vortices are no longer pinned at high fields.

Flux jumps. Flux jumps are sudden unpinning of flux vortices in response to instabilities, temperature increases, and breakdown in shielding currents as the applied field is changed. In wires with insufficient Cu or Cu-alloy stabilizer, flux jumps could lead to a quench. Flux jumps result in sudden drops in magnetization and could result in small changes in the field of a magnet.

Eddy currents. Eddy currents arise in the normal matrix material in response to a field change according to the classical mechanism dependent on the skin depth. The time constant of the eddy currents, a function of resistivity, is short. These eddy currents are differentiated from those that couple filaments, discussed above.

MAGNETIC MEASUREMENTS

The magnetic parameters of interest in evaluating multifilar Nb-Ti wire for the SSC may be obtained from measurements of magnetization as a function of field, time, and transport current. Ideally, measurements on cable samples should be also obtained. For a useful analysis, it is necessary to know the critical current density of the wire at several fields. In addition, the wire should be characterized by filament diameter, filament spacing, filament twist pitch, number of filaments, sample volume, and matrix-to-superconductor volume ratio. Magnetization values are usually reported per unit volume of superconductor or of total composite.

Magnetization in filamentary superconductors is the signal from superconductor shielding currents and other matrix currents discussed above. The magnetization-field cycle, or hysteresis loop, should have a variable cycle time, up to several hours, to extract time-dependent coupling information. The field should be transverse to the wire axis and cycle from zero to positive value. Additional information may be obtained from longitudinal-field measurements. Transport current could be controlled independently of the applied field, though in actual SSC operation the current would be approximately proportional to the field.

Total magnetic loss is the area enclosed by the loop in the magnetization-field plane. In the limit where coupling currents have decayed, the remaining area represents the magnetic hysteresis. The width of the loop at relatively high fields may be used to compute an "effective" filament diameter,[12] according to the Bean model,[13] if the critical current density is known. If coupling currents have not decayed or if filaments are coupled by the proximity effect, a large loop area will result.

Magnetization vs. Field

Several methods of magnetometry might be used for the magnetization measurements: integrated-flux, vibrating-sample (VSM), vibrating-coil (VCM), SQUID, and Hall-probe. We will discuss their advantages and disadvantages. To our knowledge, VCM and Hall-probe magnetometers have not been used for magnetic measurements of superconductors. They may be well suited for this task in a wire-fabrication environment.

Integrated-flux. This method[14,15] is good for measurements on wires carrying transport current. It detects flux jumps and frequency dependence. It requires large samples to increase the signal-to-noise ratio. Integration instrumentation limits the measurement to relatively fast field cycles.

VSM. Vibrating-sample magnetometer measurements are made with the vibration axis longitudinal[16] or transverse[17] to the field. This method is sensitive to small samples. It is a dc measurement when the field is stepped and the signal is allowed to stabilize. However, if synchronous detection is used or if the pick-up coils are well matched, data may be taken while sweeping the field. It is difficult to vibrate samples with current leads attached. We calibrate the pick-up coils with Ni wires, plates, cylinders, or spheres in the same configuration as the superconductor samples.

VCM. A vibrating-coil magnetometer[18,19] would be good for measurements on samples carrying transport current because the sample remains stationary. As with a VSM, the VCM may be used in stepped or swept fields. A wire sample could be formed into a coil, noninductively wound to avoid a magnetic signal from the transport current in the sample. As with a VSM, the field is supplied by an external magnet. The applied field should be uniform to avoid field-induced signals. Calibration would be similar as for a VSM.

SQUID. This method[20,21] is extremely sensitive and precise, suited to small samples. Any current to the sample would disrupt the SQUID circuitry. Field cycles are extremely slow.

Hall-probe. Two calibrated, cryogenic probes are used, one to measure the applied field, the other to measure the flux density at the sample surface.[22-24] The difference is the sample magnetization (after correcting for demagnetizing field, if necessary). The Hall probe could be positioned so the Hall element is parallel to the azimuthal magnetic field from the current, but perpendicular to the magnetic field and the magnetic moment from the superconducting shielding currents. This method would be appropriate for cable samples. Calibration may be achieved as for a VSM.

AC Susceptibility vs. Temperature

AC susceptibility is usually measured as a function of temperature in constant ac field, with or without a dc bias field. Measurements are made with a coaxial mutual-inductance system consisting of a primary excitation field coil, a secondary pick-up coil, and a secondary compensation coil.[25,26] Susceptibility is an excellent tool for determining critical temperatures and proximity-effect coupling in fine-filament superconductors.[27] Low frequencies are used to avoid eddy currents in the normal-metal matrix.

STUDY OF PROTOTYPE SSC WIRES AND CABLES

A disconcerting problem in accelerator magnets is field change over several hours at constant magnet current. This is often expressed as instability in multipole fields.[1,8,9] Possible mechanisms are flux creep and eddy-current coupling between filaments. If the mechanism is flux creep, there are two possibilities. One is flux creep intrinsic to the Nb-Ti superconductor filaments or their surface. The other is flux creep in the proximity-coupled matrix. (The proximity coupling itself is not time dependent.) The presence of proximity-effect coupling in filamentary superconducting wire may be deduced from measurements of magnetization vs. field or magnetic susceptibility vs. temperature.

Proximity-Effect Coupling

In hysteresis loops of magnetization vs. field, proximity coupling causes a magnetization peak centered near zero field.[28,29] (The exact position depends on a demagnetization correction of the field axis.) This peak is different from the peak in the second and fourth quadrants which is seen experimentally and predicted by the Kim model for critical current density.[30] The coupling peak arises from a large effective filament diameter when filaments are coupled at low field. The proximity coupling is destroyed at fields greater than about 0.2 T.

In ac susceptibility measurements, a large coupling peak in the imaginary part may be seen as a function of temperature. This peak represents hysteresis loss when the lower critical field of the proximity-coupled matrix becomes on the order of the measuring field as temperature increases. Thus, the peak temperature is a strong function of measuring field amplitude. We have used this technique to study intergranular coupling in high-temperature superconductors.[31]

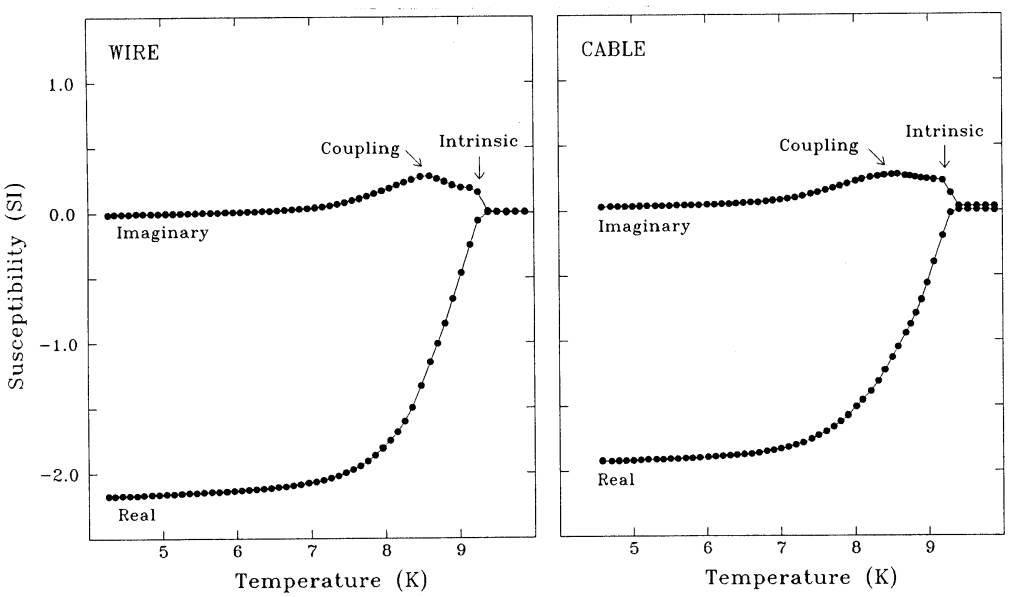

Fig. 1. AC susceptibility (uncorrected for demagnetization factor) vs. temperature measured at 0.1 mT rms at 10 Hz for wire and cable samples. The imaginary part shows intrinsic and coupling loss peaks. The real part shows a broad transition which includes intrinsic and coupling transitions.

Figure 1 shows the real and imaginary parts of external (not corrected for demagnetization factor) ac susceptibility as functions of temperature for samples consisting of small, sawed segments of prototype SSC wire and cable with 0.5% Mn in the Cu matrix. The filament diameter is 5.3 μm and the filament spacing is 0.53 μm. The susceptibility is plotted per unit volume of Nb-Ti. The measuring field was 0.1 mT rms at 10 Hz applied perpendicular to the wire and cable axes. The cable was the type used in the fabrication of the inner layer of dipole magnet D-15A-6 in Ref. 1.

Intrinsic and coupling loss peaks (partially overlapping) appear in the imaginary part of susceptibility. Correction for demagnetization factor would change the apparent shapes of the peaks. For a measuring field of 0.01 mT, the coupling peaks move to higher temperature. For a 1-mT field, the peaks are well separated as the coupling peaks move to lower temperature. Much less pronounced susceptibility peaks were seen for fields applied parallel to the wire and cable axes. But similar coupling peaks in the imaginary part were seen for wire and cable used for the outer layer of dipole magnet D-15A-6. The filaments are coupled at low temperature for low fields despite the Mn doping of the matrix. As expected, magnetization vs. field at 4 K showed characteristic coupling peaks near zero field.

Multipole-field instability occurs at the relatively high fields that would destroy proximity-effect coupling. However, there are portions of a dipole magnet which are exposed to very small fields where coupling is presumably intact. In multifilamentary wires that are proximity coupled, flux creep *may* occur in the interfilamentary matrix. We recently proposed this mechanism to explain subtle intergranular frequency effects in the ac susceptibility of high-temperature superconductors.[32] To inhibit low-field proximity coupling, more Mn could be added to the matrix, or a resistive Cu-Ni matrix could be used.

Intrinsic Flux Creep

In addition to the possibility of flux creep in the proximity-coupled matrix, there may be intrinsic flux creep in the superconducting filaments. Flux creep[10] has been observed in Tevatron cable made with wire containing presumably decoupled filaments separated by approximately 3 μm.

We measured positive-field VSM hysteresis loops for a small segment of D-15A-6 outer-layer cable, filament diameter 4.3 μm and filament spacing 0.43 μm, to see if there were time effects. The maximum field was 1 T, high enough to uncouple the filaments, perpendicular to the cable axis and parallel to the wide side. The field was stepped in units of 50 mT. For one cycle, magnetization was recorded after waiting 30 seconds after a field change. The wait time was 3 minutes for the other cycle. There was no significant difference in the hysteresis loops. This suggests an absence of intrinsic flux creep *on the time scale of these measurements*.

Eddy-Current Filament Coupling

If multipole-field instability arises from eddy-current filament coupling, more twist per unit length would help alleviate it. However, because the coupling currents decay quickly in the resistive matrix,[33] they should not be a factor for the drift of multipole fields over a period of hours.

To check for this time-dependent effect, we measured hysteresis loops, using the two field cycles described above, for two coiled samples of D-15A-6 wire used in the inner- and outer-layer cables. The field was applied along the axis of the coils, approximately transverse to the wire axis. These particular samples had 0.5 and 1.5 twists per centimeter, respectively,

verified by etching in nitric acid the matrix of companion samples. Unlike the short cable segment described above, the length of wire for each coil sample was about 25 cm, long enough to contain many twists. There were no differences between long and short field cycles for the two coils. The result suggests that 0.5 twist per centimeter is adequate to inhibit eddy-current filament coupling for these wait times.

CONCLUSIONS

We have discussed several magnetic parameters to be considered in testing multifilar Nb-Ti superconductor for the SSC, with the goal of minimizing field nonuniformity, field instability, large residual fields, and large energy losses. These parameters may be extracted from measurements of magnetization vs. field. Several measurement methods, each with certain advantages, were described.

Measurements of ac susceptibility of candidate SSC wires and cables demonstrate proximity-effect coupling. Flux creep in the proximity-coupled matrix may be a source of time variations of multipole fields in prototype SSC magnets. Intrinsic flux creep was not observed over a period of minutes. Wires used for the inner and outer layers of the D-15A-6 prototype SSC dipole magnet did not show serious eddy-current filament coupling for these sample twist pitches.

ACKNOWLEDGMENTS

We had helpful discussions with C. E. Taylor, R. M. Scanlan, W. S. Gilbert, E. W. Collings, and D. C. Larbalestier. R. J. Loughran assisted with the VSM measurements. Sample wires and cables were generously provided by R. M. Scanlan. This work was supported by the Department of Energy, Division of High Energy Physics.

REFERENCES

1. W. S. Gilbert, R. F. Althaus, P. J. Barale, R. W. Benjegerdes, M. A. Green, M. I. Green, and R. M. Scanlan, Magnetic field decay in model SSC dipoles, *IEEE Trans. Magn.* **25**:1459 (1989).
2. Y. B. Kim, C. F. Hempstead, and A. R. Strnad, Magnetization and critical supercurrents, *Phys. Rev.* **129**:528 (1963).
3. M. N. Wilson, "Superconducting Magnets," Oxford University Press, Oxford, U.K. (1983), pp. 171-174.
4. *Ibid.*, pp. 139-140, pp. 194-197, p. 308.
5. L. F. Goodrich and S. L. Bray, Current capacity degradation in superconducting cable strands, *IEEE Trans. Magn.* **25**:1949 (1989).
6. E. W. Collings, Stabilizer design considerations in fine-filament Cu/NbTi composites, *Adv. Cryo. Engr. (Materials)* **34**:867 (1988).
7. G. H. Morgan, Theoretical behavior of twisted muticore superconducting wire in a time-varying uniform magnetic field, *J. Appl. Phys.* **41**:3673 (1970).
8. D. A. Herrup, M. J. Syphers, D. E. Johnson, R. P. Johnson, A. V. Tollestrup, R. W. Hanft, B. C. Brown, M. J. Lamm, M. Kuchnir, and A. D. McInturff, Time variations of fields in superconducting magnets and their effects on accelerators, IEEE Trans. Magn. **25**:1643.
9. R. W. Hanft, B. C. Brown, D. A. Herrup, M. J. Lamm, A. D. McInturff, and M. J. Syphers, Studies of time dependence of fields in Tevatron superconducting dipole magnets, *IEEE Trans. Magn.* **25**:1647.
10. M. Kuchnir and A. V. Tollestrup, Flux creep in a Tevatron cable, *IEEE Trans. Magn.* **25**:1839.

11. P. W. Anderson and Y. B. Kim, Hard superconductivity: Theory of the motion of Abrikosov flux lines, *Rev. Mod. Phys.* **36**:39 (1964).
12. S. S. Shen, Magnetic properties of multifilamentary Nb_3Sn composites, *in:* "Filamentary A15 Superconductors," M. Suenaga and A. F. Clark, eds., Plenum, New York (1980), pp. 309-320.
13. C. P. Bean, Magnetization of high-field superconductors, *Rev. Mod. Phys.* **36**:31 (1964).
14. W. A. Fietz, Electronic integration technique for measuring magnetization of hysteretic superconducting materials, *Rev. Sci. Instrum.* **36**:1621 (1965).
15. M. N. Wilson, *op. cit.*, pp. 243-245.
16. P. J. Flanders, Instrumentation for magnetic moment and hysteresis curve measurements, *in:* "Conference on Magnetism and Magnetic Materials," American Institute of Electrical Engineers, New York (1957), T-91, pp. 315-317.
17. S. Foner, Versatile and sensitive vibrating-sample magnetometer, *Rev. Sci. Instrum.* **30**:548 (1959).
18. D. O. Smith, Development of a vibrating-coil magnetometer, *Rev. Sci. Instrum.* **27**:261 (1956).
19. K. Dwight, N. Menyuk, and D. Smith, Further development of the vibrating-coil magnetometer, *J. Appl. Phys.* **29**:491 (1958).
20. E. J. Cukauskas, D. A. Vincent, and B. S. Deaver Jr., Magnetic susceptibility measurements using a superconducting magnetometer, *Rev. Sci. Instrum.* **45**:1 (1974).
21. J. A. Good, A variable temperature high sensitivity SQUID magnetometer, *in:* "SQUID: Superconducting Quantum Interference Devices and their Applications," H. D. Hahlbohm and H. Lübbig, eds., Walter de Gruyter, Berlin (1977), pp. 225-238.
22. D. A. Berkowitz and M. A. Schippert, Hall effect B-H loop recorder for thin magnetic films, *J. Sci. Instrum.* **43**:56 (1966).
23. D. J. Craik, The measurement of magnetization using Hall probes, *J. Phys. E: Sci. Instrum.* **1**:1193 (1968).
24. P. J. Flanders, A Hall sensing magnetometer for measuring magnetization, anisotropy, rotational loss and time effects, *IEEE Trans. Magn.* **21**:1584 (1985).
25. W. R. Abel, A. C. Anderson, and J. C. Wheatley, Temperature measurements using small quantities of cerium magnesium nitrate, *Rev. Sci. Instrum.* **35**:444 (1964).
26. R. B. Goldfarb and J. V. Minervini, Calibration of ac susceptometer for cylindrical specimens, *Rev. Sci. Instrum.* **55**:761 (1984).
27. J. R. Cave, A. Février, H. G. Ky, and Y. Laumond, Calculation of ac losses in ultra fine filamentary NbTi wires, *IEEE Trans. Magn.* **23**:1732 (1987).
28. A. K. Ghosh, W. B. Sampson, E. Gregory, and T. S. Kreilick, Anomalous low field magnetization in fine filament NbTi conductors, *IEEE Trans. Magn.* **23**:1724 (1987).
29. E. W. Collings, K. R. Marken Jr., M. D. Sumption, R. B. Goldfarb, and R. J. Loughran, AC loss measurements of two multifilamentary NbTi composite strands, paper AY-05, this conference.
30. D.-X. Chen and R. B. Goldfarb, Kim model for magnetization of type-II superconductors, *J. Appl. Phys.* **66**:2510 (1989).
31. R. B. Goldfarb, A. F. Clark, A. I. Braginski, and A. J. Panson, Evidence for two superconducting components in oxygen-annealed single-phase Y-Ba-Cu-O, *Cryogenics* **27**:475 (1987).
32. M. Nikolo and R. B. Goldfarb, Flux creep and activation energies at the grain boundaries of Y-Ba-Cu-O superconductors, *Phys. Rev. B* **39**:6615 (1989).
33. M. N. Wilson, *op. cit.*, pp. 176-181.